The Egyptian Journal of Remote Sensing and Space Sciences 27 (2024) 555–564

Contents lists available at ScienceDirect

The Egyptian Journal of Remote Sensing and Space Sciences

journal homepage: www.sciencedirect.com

Research Paper

# Semi-automated mangrove mapping at National-Scale using Sentinel-2, Sentinel-1, and SRTM data with Google Earth Engine: A case study in Thailand

Surachet Pinkeaw [a], Pawita Boonrat [a,*], Werapong Koedsin [a,b], Alfredo Huete [a,c]

[a] Faculty of Technology and Environment Prince of Songkla University, Phuket Campus, Phuket 83120, Thailand
[b] Andaman Environment and Natural Disaster Research Center (ANED), Faculty of Technology and Environment, Prince of Songkla University, Phuket Campus, Phuket 83120, Thailand
[c] School of Life Sciences, University of Technology Sydney, NSW 2007, Australia

ARTICLE INFO

*Keywords:*
Forest Classification
Blue Carbon
Machine learning
GEE
Satellite Imaginary
Geospatial Technique
Geoinformatics

ABSTRACT

Mangroves are a crucial part of the coastal ecosystem; thus, precise and up-to-date monitoring is essential to guide regional policies and inform conservation strategies. This study investigates the capabilities of semi-automated remote sensing approaches within a Google Earth Engine framework for national-scale mangrove mapping in Thailand. Remote sensing data from 2018—10,000 data points acquired from Sentinel-1, Sentinel-2, and the Shuttle Radar Topography Mission (SRTM)—was used to train several machine learning models. The Gradient Tree Boost (GTB) proved to be the most reliable, with the least variation in validity (the lowest IQR) and the highest average Overall Accuracy of 96.75 ± 0.63 % compared to the others—96.64 ± 0.72 % for Random Forest (RF); 96.12 ± 0.80 %for Classification and Regression Trees (CART); and 95.43 ± 0.74 % for Support Vector Machines (SVM). Thus, the GTB was instrumental in mapping mangrove distribution with 10-m spatial resolution across Thailand from 2016 to 2022, the period in which the mangrove areas increased by 11 %, reflecting successful conservation efforts over the past decade. The developed framework establishes the foundation for semi-automated mangrove mapping that can be developed for other geographical contexts.

## 1. Introduction

Mangroves are found in the littoral zones of tropical and subtropical coastlines, located between land and sea at the estuary between 30°S and 30°N (Giri et al., 2011). Because they provide vital functions to coastal ecosystems, mangrove forests are important. They provide sanctuary and nourishment for marine life and species and act as a natural barrier against erosion brought on by waves and storms. Importantly, mangroves function as carbon reservoirs and are significant carbon sinks along coasts (Alongi and Mukhopadhyay, 2015; Bindu et al., 2020).

Mangrove areas have dramatically declined by human activities such as agriculture, aquaculture, shrimp ponds, land reclamation, urban settlements, and port infrastructure (Richards and Friess, 2016; Thomas et al., 2017). The decline is also accounted for by tidal waves, storm surges, and coastal erosion (Linneweber and De Lacerda, 2002; Richards and Friess, 2016). The physicochemical conditions and growth of mangrove forests are vulnerable to climate change; global warming raises the sea level and increases water salinity (Neumann, 1997; Shiau et al., 2017).

Monitoring spatial and temporal dynamics is critical for determining mangrove extent and the efficacy of restoration policies, which require high spatial resolution and temporal data. Mapping mangroves is typically resource-intensive and time-consuming, particularly for inaccessible areas (Giri et al., 2007; Zhang et al., 2014). Remote sensing has been employed to quantify a decade change in mangrove distribution on a global scale with 30-m spatial resolution the worldwide spatial distribution of mangroves, as well as their rates of change across decadal periods (Bunting et al., 2018; Giri et al., 2011; Hamilton and Casey, 2016). Nevertheless, more than such a resolution is needed for regional management.

In Thailand, the national-scale mangrove monitoring has been reported every five years (DMCR, 2023). Unfortunately, no annual report exists, nor the accessibility of geospatial data online. As a developing

* Corresponding author.
*E-mail address:* pawita.b@phuket.psu.ac.th (P. Boonrat).

https://doi.org/10.1016/j.ejrs.2024.07.001
Received 9 October 2023; Received in revised form 28 June 2024; Accepted 4 July 2024
Available online 8 July 2024

country, Thailand requires monitoring tools that are convenient to use and easily replicable while maintaining accuracy in mapping. Google Earth Engine (GEE) is a free cloud-based platform for global-scale geospatial analysis that runs on Google's cloud (Gorelick et al., 2017). Its catalogue provides access to various satellite data and remote sensing products, including a range of packages from advanced image processing to machine learning algorithms. GEE has been employed for numerous applications: hydrology, urban planning, natural catastrophe analysis, and land use and land cover (Amani et al., 2020; Gorelick et al., 2017). Several applications were for mangrove monitoring in various scales (Cissell et al., 2021; Ghorbanian et al., 2021; Hu et al., 2020; Mandal and Hosaka, 2020; Zhao and Qin, 2022).

GEE can be applied as a semi-automated mapping that combines automated tools with manual refinement to produce accurate and dependable maps. It balances the efficiency of automated methods when dealing with large amounts of data with the precision of human expertise. The combination ensures the quality and validity of the mapping output, providing an advantage over solely automated or manual methods. Example applications of GEE semi-automated mapping are: land use and land cover (Mack et al., 2017); topography mapping of intertidal zones (Sharma et al., 2021); and oil palm landcover classification (Sarzynski et al., 2020). To our knowledge, there needs to be a sufficient model available for semi-automated mapping of mangroves that is both robust and sustainable.

The GEE environment allows the analysis of satellite images from Sentinel-2, Sentinel-1, and the Shuttle Radar Topography Mission (SRTM). These three satellites each offer unique advantageous features, and their combined use yields mutually beneficial advantages. Sentinel-2 has the capability of providing imagery across various spectral bands. Sentinel-1 offers valuable imagery in particular bands in additionally to Sentinel-2. Both Sentinel-1 and Sentinel-2 are distinguished from other open-source satellites by their exceptional spatial resolution of 10 m. SRTM, despite its comparatively lower spatial resolution of 30 m, provides elevation information that especially benefits analyses of mangrove ecosystems where elevations are often significant.

Several machine learning algorithms are enabled to be performed on the GEE platform. The most frequently used algorithms for supervised pixel-based classification are Random Forest (RF), Classification and Regression Trees (CART), and Support Vector Machines (SVM) (Taminia et al., 2020). Gradient Tree Boost (GTB) has emerged for mangrove classification in recent years, i.e., seasonal leaf nutrients mapping (Miao et al., 2022), and estimation of above-ground biomass (Pham et al., 2020; Singh and Mahajan, 2023).

CART is a standard single-tree decision model where the data are classified for the attribute maximising the information gain. It is a rapid, simple and highly flexible algorithm (Ouma et al., 2022; Pal and Mather, 2003). SVM minimises misclassification and optimizes a hyperplane that splits the data into two classes. SVM stands out for its capacity to manage large-dimensional classification problems with small sample sizes (Hu et al., 2018). RF is an ensemble of numerous independently-trained decision trees (Cutler et al., 2007). RF can overcome overfitting (Shelestov et al., 2017), manage high-dimensional data, and discover nonlinear relationships (Breiman, 2001). GTB uses gradient descent to minimise the loss function in order to strengthen ensembles of weak learner trees iteratively (Friedman, 2002). It can capture complex data relationships without overfitting (Ouma et al., 2022).

For the above reason, this study investigates the potential of the semi-automated model—requiring manual assistance for preparing the input data, while the remaining processes are automated—in mangrove mapping on a national scale in Thailand. The remote-sensing data used are in the GEE environment, i.e., Sentinel-2, Sentinel-1, and SRTM. The objectives are (i) to identify an adequate machine learning model (among CART, SVM, RF, and GTB) for classifying mangrove areas using GEE and (ii) to quantify the change in mangrove areas during 2016–2022.

The novelty of our research lies in the development of a semi-automatic mapping model tailored for Thailand, characterised by the combination of high-resolution satellite time series with a spatial resolution of up to 10 m. This model is made feasible through complimentary access to free-of-charge satellite data on the GEE platform. This development is an important step forward for ecological mapping, especially for accurate mangrove ecosystem monitoring.

## 2. Materials and methods

### 2.1. Study area

This study focuses on the national scale of Thailand, specifically examining the country's mangrove area. Initially, we employed the mangrove boundary obtained from the Royal Thai Government in 2000 through a Cabinet Resolution from the Department of Marine and Coastal Resources (DMCR) (DMCR, 2021a). The classification area refers to a designated region outlined by the boundary and further enclosed by a 2 km buffer zone from the original border, as depicted in Fig. 1. The mangrove covers are located across 24 provinces of Thailand, mostly in the lower Andaman Sea, followed by the upper Andaman Sea and the Gulf of Thailand (DMCR, 2021a, 2021b). The latest report is of 2019, when mangroves covered 2,779.23 $km^2$, an increase of 323.90 $km^2$ compared to the prior report in 2014 (DMCR, 2021b).

### 2.2. Data pre-processing

#### 2.2.1. Remote sensing data

Sentinel-2, Sentinel-1, and SRTM data (from 2016 to 2022) available on GEE were used. Sentinel-2 data was utilised for the Enhanced Vegetation Index (EVI), Mangrove Vegetation Index (MVI), visible wavelengths (B2, B3, B4), the first red-edge band (B5), near-infrared (NIR; B8A), and short-wave infrared 1 (SWIR1; B11). The VH polarisation band was obtained from Sentinel-1. SRTM provided digital elevation data. These diverse datasets served as crucial variables in our classification algorithm, facilitating the creation of comprehensive mangrove forest maps for Thailand from 2016 to 2022. The details are described as follows:

(i) Sentinel-2 Satellite Imagery

Sentinel-2 Satellite's product used was the Multi-Spectral Instrument (MSI) Level-1C orthorectified top-of-atmosphere reflectance products. It includes 13 spectral bands with spatial resolutions ranging from 10 m to 60 m (Table S1). Although archived from 23 June 2015 to the present, the 2015 data was unavailable for the study area, prompting the use of 2016–2022 images. The selection process began with satellite photos with less than 25 % cloud cover. A reduced image collection was made by taking the median of all values at each pixel in the stack of bands corresponding to the image. From 25 January 2022, scenes from Sentinel-2 with a processing baseline of '04.00′ or higher experienced a shift in their Digital Number (DN) value range by 1000. To maintain consistency, harmonised Sentinel-2 MSI images were employed for the 2022 classification.

Band selections of Sentinel-2 were carried out based on previous studies. Bands 2–5 were chosen as the visible wavelengths in the spectral signature of plant pigments can be used to distinguish tree-covered regions from other types of land cover (Yang et al., 2022). The NIR region helps to inform vegetation characteristics, such as leaf pigments, cellulose (Yang et al., 2022), plant greenness (Huete, 2004), leaf moisture, or water content (Baloloy et al., 2020; Tian et al., 2010). Mangroves have more water stored in their leaves and canopy than most terrestrial forests, thus reflecting the infrared less than other forests (Yang et al., 2022). SWIR and the red-edge band are also useful for plant classification (Immitzer et al., 2016) as well as for detecting phenological differences (Persson et al., 2018). Previous studies reported that the SWIR and the first Red-edge (B5) were the most relevant for the plant

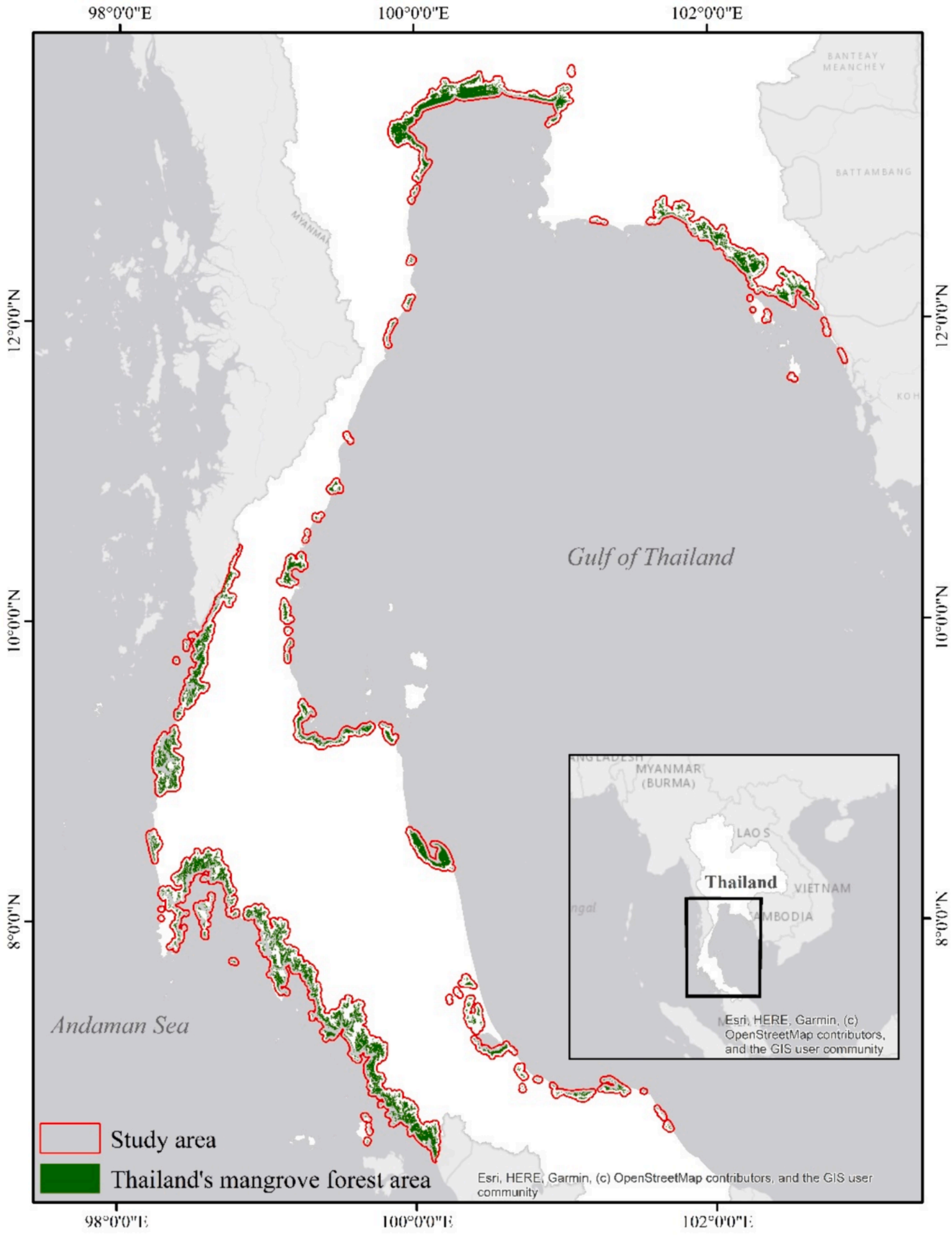


**Fig. 1.** Study area depicting mangrove forests in Thailand. The 2 km buffered area (outlined in red) is based on the 2000 Cabinet Resolution of the Royal Thai Government, with DMCR-defined mangroves shown in green. (For interpretation of the references to color in this figure legend, the reader is referred to the web version of this article.)

classification (Macintyre et al., 2020; Ramoelo et al., 2015) as they are associated with the chlorophyll content (Fernández-Manso et al., 2016; Sun et al., 2020). The red edge is helpful in estimating biomass and crop yield (Wu et al., 2019). Mangroves reflect SWIR reflected by mangroves is different from other vegetation (Hu et al., 2020; Yang et al., 2022). For the above reasons, this study employed the visible wavelengths (B2, B3, B4), first Red-edge (B5), NIR (B8A; a narrow range in NIR), and SWIR1 (B11) for the classification of mangrove forests (see Asterisks marked

bands in Table S1).

The vegetation indices employed in this study are the Enhanced Vegetation Index (EVI) and the Mangrove Vegetation Index (MVI):

$$EVI = 2.5 \times \frac{NIR\text{-}RED}{NIR + 6.0RED - 7.5BLUE + 1} \quad (1)$$

$$MVI = \frac{NIR - GREEN}{SWIR1 - GREEN} \quad (2)$$

where NIR, RED, GREEN, BLUE, and SWIR1 are the near-infrared (B8), red (B4), green (B3), blue (B2), and shortwave-infrared (B11) reflectance of Sentinel-2 bands, respectively.

EVI is generally used for vegetation discrimination, biomass estimation, health, and greenness; EVI has reported to overcome the saturation challenge under high vegetation cover (Huete et al., 2002; Liu and Huete, 1995). EVI is suitable for mangrove time-series analysis as it can distinguish the interior of forest areas with high clarity (Zhu et al., 2021). MVI derived from remote sensing images was demonstrated for rapid and precise mapping of mangrove boundaries, effectively highlighting the greenness and the moisture of the forests information in mangroves (Baloloy et al., 2020).

(ii) Sentinel-1 Satellite Imagery

Sentinel-1's product, the dual-polarization C-band Synthetic Aperture Radar (SAR) Ground Range Detected (GRD), were utilised, having a 10-mspatial resolution and four polarisation bands (VV, HH, VV + VH, and HH + HV) (see Table S2). The scene was pre-processed via the Sentinel-1 Toolbox, using SRTM 30 or ASTER DEM, with the following corrections: Thermal noise removal; Radiometric calibration; and Terrain correction. The VH polarisation was used to classify mangrove forests since the plant canopy structure is responsive to the VH band (Chauhan and Srivastava, 2016). Sentinel-1 images were selected during 2016–2022. A filter was conducted to obtain images collected in interferometric wide swath mode and produce a composite from median polarisation.

(iii) Shuttle Radar Topography Mission (SRTM)

This study utilised elevation data, a crucial factor in the classification of mangrove forests (Zhao and Qin, 2020). The data was acquired from SRTM of NASA Jet Propulsion Laboratory's (NASA JPL) SRTM V3 product (SRTM Plus), commonly known in GEE as the NASA SRTM Digital Elevation 30 m; it is a digital elevation model with a 30-mspatial resolution.

#### 2.2.2. Geographic information system data (GIS data) and sampling points

The boundaries for mangrove and non-mangrove areas were sourced from (i) the land used data from Thailand's Land Development Department and (ii) the forest data from the Royal Forest Department. Both data were in a shapefile format. The mangrove areas intersected the annual land use data from 2016 to 2018 and the annual forest data in 2018. The non-mangrove areas were obtained by intersecting the six sub-classes of land use data (i.e., terrestrial forests, agriculture, aquaculture, built-up/urban, bare land/sand, and water/sea) of two periods (2016–2018 and 2019–2021). The sample points were obtained via a random stratification; the non-mangroves' were the combination of points sampled from each sub-class. The sample points were randomly selected at 10,000 in each class for mangrove and non-mangrove areas.

### 2.3. Mangrove forest classification

#### 2.3.1. Classification algorithms

This study compared five classification algorithms that have previously been utilised for mangrove mapping: (i) CART (Giri et al., 2014; Li et al., 2019; Mandal and Hosaka, 2020; Mondal et al., 2019); (ii) SVM (Cao et al., 2018; Li et al., 2019; Toosi et al., 2019; Xia et al., 2018); (iii) RF (Cissell et al., 2021; Ghorbanian et al., 2021; Hu et al., 2020; Li et al., 2019; Mondal et al., 2019; Toosi et al., 2019; Zhao and Qin, 2020); (iv) GTB (Baviskar and Dhiman, 2022; Liu et al., 2021). The relevant parameters assigned in this study are listed in Table S4.

#### 2.3.2. Accuracy assessment and statistical analysis

The salt-and-pepper noise caused by misclassified pixels was minimised via the morphological reducer filter; the values of isolated pixels are replaced by the surrounding pixels. A square kernel of a 30-m width was applied in the post-classification process. Each class of the sample—mangrove (10,000 points) and non-mangrove (10,000 points)—was split into a 50:50 ratio into the train set (5,000 points) and the test set (5,000 points). The resulting non-mangrove areas were cross-checked visually via the Open Street Map and Google Earth.

The confusion matrix was used to assess the model's accuracy. The overall accuracy (OA) and Kappa coefficient (Kappa) (Cohen, 1960) were retrieved annually. The average OAs and Kappas for the observed period of the performed models were compared. The annual OAs obtained from each model were further examined via the one-way analysis of variance (One-way ANOVA). This hypothesis test considers only one categorical variable or factor (Brown and Forsythe, 1974). The annual OAs are significantly different when p-value $< 0.05$. The model with the highest averaged OA outperforms the others. All methodological procedures can be summarised in a flowchart diagram, as shown in Fig. 2.

## 3. Results and discussion

### 3.1. Results of mangrove forest classification

The EVI, MVI, visible wavelengths (B2, B3, B4), the first red-edge band (B5), NIR (B8A), and SWIR1 (B11) were all calculated using Sentinel-2 data. Sentinel-1 provided the VH polarisation band. Digital elevation data was supplied by SRTM. The combined datasets were essential factors in our classification model to generate detailed maps of Thailand's mangrove forests from 2016 to 2022.

All models, namely CART, SVM, RF, and GTB, successfully classified mangrove and non-mangrove areas during 2016–2022 with OAs greater than 94 % and Kappas exceeding 0.80 (see Table S5). This indicated that all performed algorithms can be used for mangrove classification. GTB has the highest average OA (96.75 ± 0.63 %). In addition, GTB delivered higher OA and Kappa values than the others in each year except for 2018, where it performed equally well as RF.

The highest OA achieved by GTB in this study is in line with previous works. Baviskar and Dhiman (2022) discovered that GTB outperformed CART, RF, and SVM when studying the spatiotemporal assessment of mangrove ecosystems in Coastal Megacity, Mumbai, India. Miao et al. (2022) found that XGBoost—a model developed from GTB—performs more accurately estimating mangrove leaf nutrients than other approaches (RF, light gradient boosting machine, and extreme gradient boosting).

The high accuracies of RF also align with several studies. Mondal et al. (2019) found that RF surpasses CART and SVM in mangrove mapping in West Africa and found that using RF and CART. Toosi et al. (2019) also reported that RF outperformed other algorithms (RF, Regularized Discriminant Analysis, Least Squares SVM Radial, and Linear SVM) in monitoring mangrove cover changes in southern Iran.

Hence, GTB was concluded to be the most efficient, followed by RF. The authors also suggest the development of GTB, such as XGBoost (available in Python programming), to improve efficiency in mangrove classification in future studies.

Fig. 3a illustrates the nation's largest mangrove area, which is in Phang-Nga Bay, derived from the data in 2018. Fig. 3b-c are the corresponding true-colour and false-colour composites of satellite images. Fig. 3d-g compares the models' performances.

Some terrestrial forests were misclassified as mangrove forests via

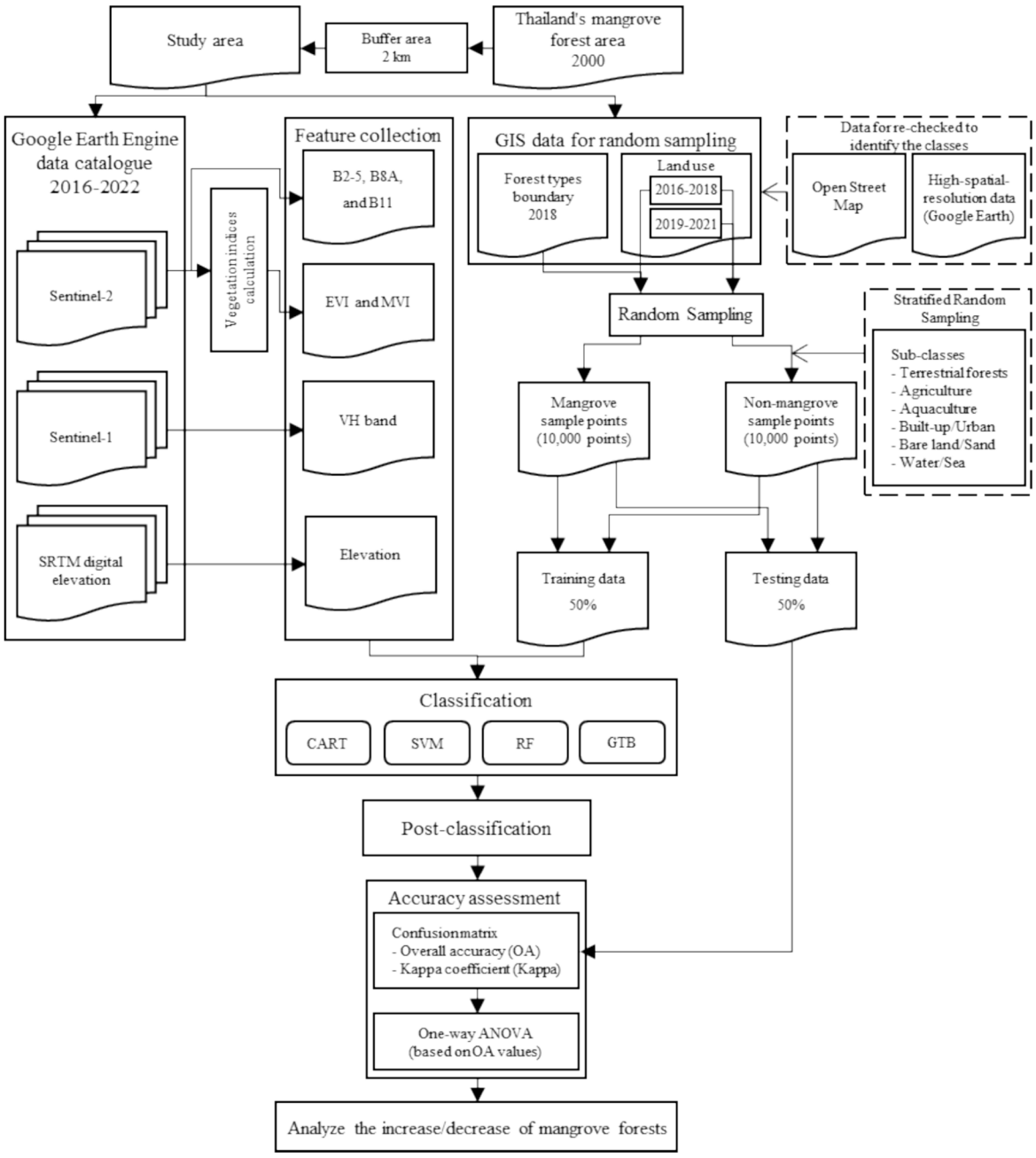


**Fig. 2.** Flow chart detailing the mangrove forest classification process.

CART (Fig. 3d) and SVM (Fig. 3e), whereas RF (Fig. 3f) and GTB (Fig. 3g) are accurately classified. This misclassification is likely due to the region's topography featuring mountains proximate to mangrove areas and inland forests adjacent to hills (yellow frames). The geographical closeness may influence the misclassifications, with shadows and reflection angles playing pivotal roles.

Furthermore, it was demonstrated that some aquaculture areas related to agricultural areas (pink frames) were incorrectly classified as mangrove forests, particularly by the CART and SVM classifications for agricultural areas relative to water or rivers (red frames). It was found that some agricultural pixels were classified as mangrove forests by the CART and SVM classifications, especially the SVM (Fig. 3e). While RF and GTB had smaller amounts of misclassifications in agricultural areas than in CART and SVM.

Although the results showed that GTB has the highest average accuracy (Table S5), they also found that the accuracies were relatively close together (95.43–96.75 %), and the variations were relatively low. Therefore, the box plot and ANOVA were analysed. The distribution analysis of OA in each algorithm is shown in Fig. 4 and Table S6. The results demonstrated that RF and GTB have similar accuracy and a higher range of accuracy (both mean and median values) than CART and SVM.

A one-way ANOVA (Table S7) was used to analyse the significant differences in OA values between each method. The results showed that the OA of each algorithm was significantly different (P-value = 0.02, less than 0.05 ($P < 0.05$)). It means that GTB achieved significantly higher accuracy than other machine learning techniques. In addition, the deviation of the GBT model was lower than other models when applied to other years (2016–2017 and 2019–2022). The accuracy is only slightly different (Table S5). The result shows the robustness of the GBT model. Therefore, GTB was utilised to create the mangrove forest map in Thailand. The area of the mangrove forest in each year (2016–2022) will

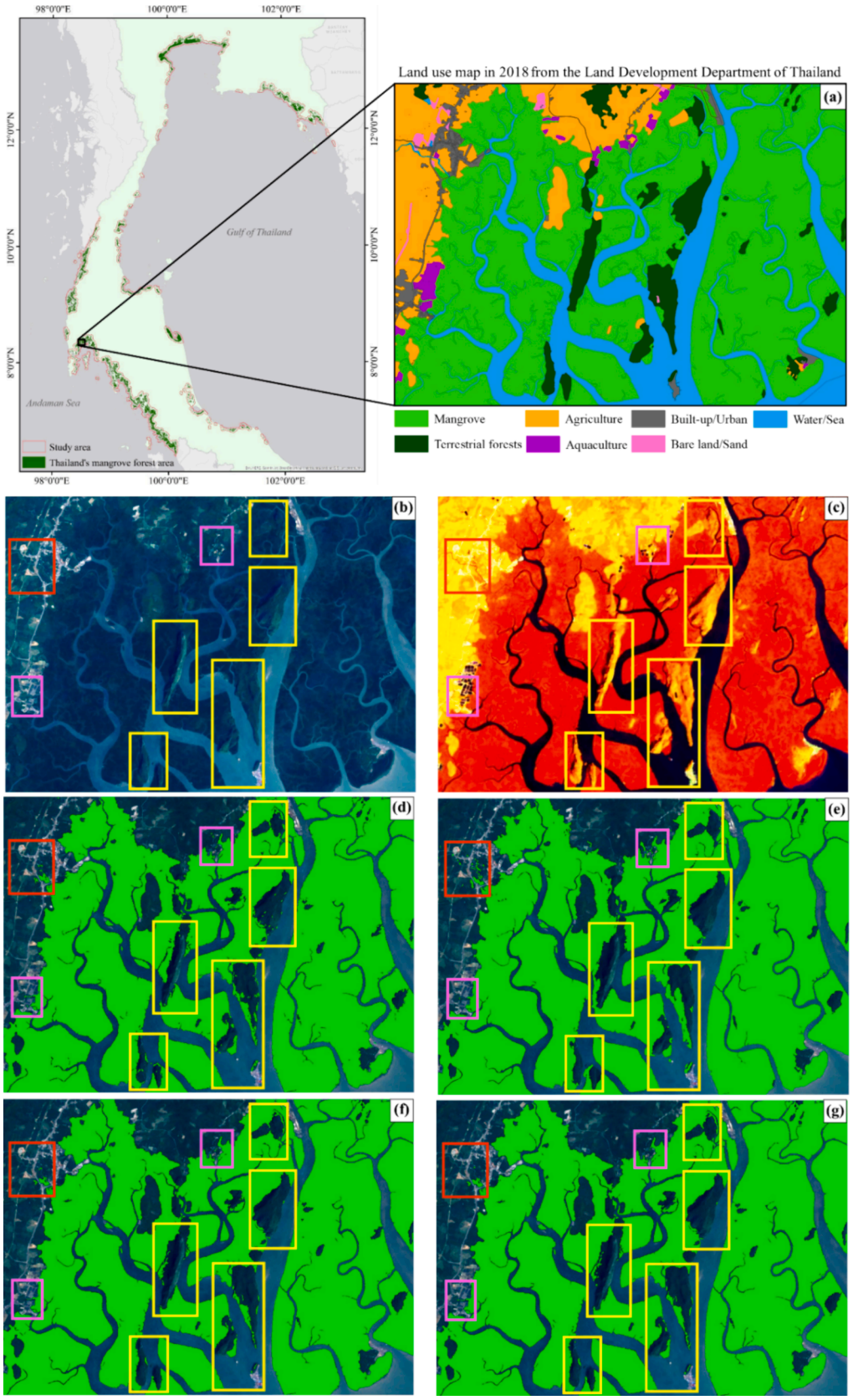


**Fig. 3.** Classification results for 2018: (a) land use map, (b) true colour composite satellite images (B4, B3, B2), (c) false color composite (B8A, B11, B4), followed by algorithm-derived classifications: (d) CART, (e) SVM, (f) RF, and (g) GTB. Key areas of interest for mangrove classification comparison include terrestrial forests near hills (yellow frames), aquaculture and agricultural zones (pink frames), and intersections of agriculture with water/river areas (red frames). (For interpretation of the references to color in this figure legend, the reader is referred to the web version of this article.)

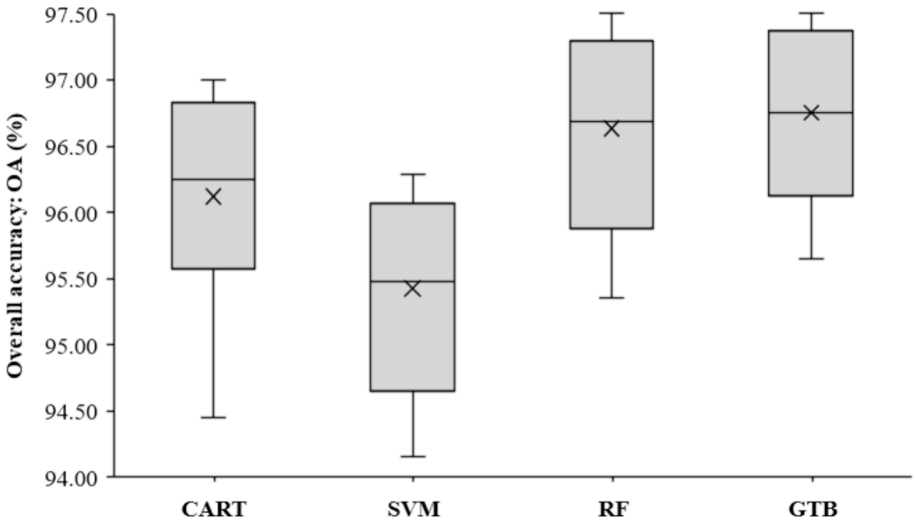


**Fig. 4.** Box plot comparing the Overall Accuracy (OA) of the four algorithms used for mangrove classification between 2016 and 2022.

be further analysed.

### 3.2. Mangrove forest area of Thailand in 2016–2022

Given the superior classification accuracy, GTB was employed to locate mangroves in Thailand from 2016 to 2022. A bar chart in Fig. 5 shows the fluctuating change in the mangrove area over these seven years, initiating with 2,455 $km^2$ in 2016. The nation experienced almost 10 % increase in mangrove coverage within a year before undergoing a reduction of approximately 7 % over the next three years. However, between 2020 and 2022, there was a rebound, with a 9 % gain in mangrove areas, culminating in 2,716 $km^2$. This translates to an overall increase of 261 $km^2$ or 11 % from 2016 to 2022. The significant improvements are Talumphuk Cape in Nakhon Si Thammarat Province, as illustrated in Fig. 6.

Such gains reflect the efficacy of the policies outlined by the National Economic and Social Development Plan—which aim for an annual increment of 8 $km^2$ from 2012 to 2016 (The National Economic and Society Development Board, 2011) and an expansion of 80 $km^2$ between 2017 and 2021 (The National Economic and Society Development Board, 2016).

In addition, governmental initiatives have implemented mangrove and beach restoration projects—including mangrove planting and promoting people's participation in the conservation and care of the ecosystem (The Ministry of Natural Resources and Environment, 2021). These initiatives are within the conceptual framework constituting the 20-year Master Plan of the Ministry of Natural Resources and Environment (2018–2037), as declared in the Cabinet's Policy 10, focusing on Natural Resources Regeneration and Environmental Protection for Sustainable Growth, presented to the National Assembly in 2019 (The Ministry of Natural Resources and Environment, 2021).

There are several benefits and limitations to our research that should be considered. The novelty of our research is in developing a semi-automatic mapping model tailored for Thailand, characterised by the combination of high-resolution satellite time series with a spatial resolution of up to 10 m. The model uses publicly available satellite data and GEE. Our research does have some significant limitations, though. Firstly, the model's application is currently confined to Thailand. The accuracy of this model may vary depending on the location due to variations in species mix and environmental factors. Secondly, significant changes in land use within non-mangrove areas could restrict the model's applicability. These modifications may significantly impact the reflectance patterns that the model depends on. As the machine learning parameters used in this study were set as the default parameters, the

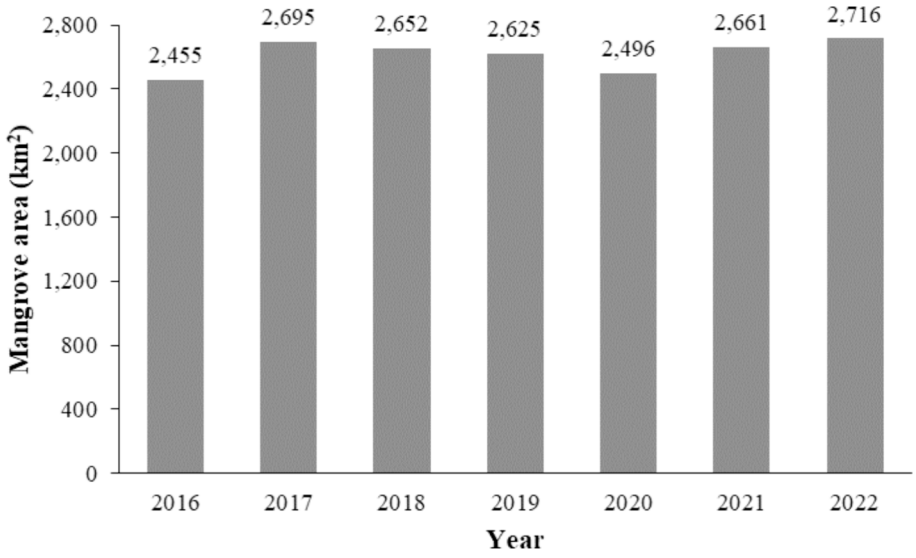


**Fig. 5.** Mangrove forest coverage in Thailand from 2016 to 2022, as classified by the GTB algorithm.

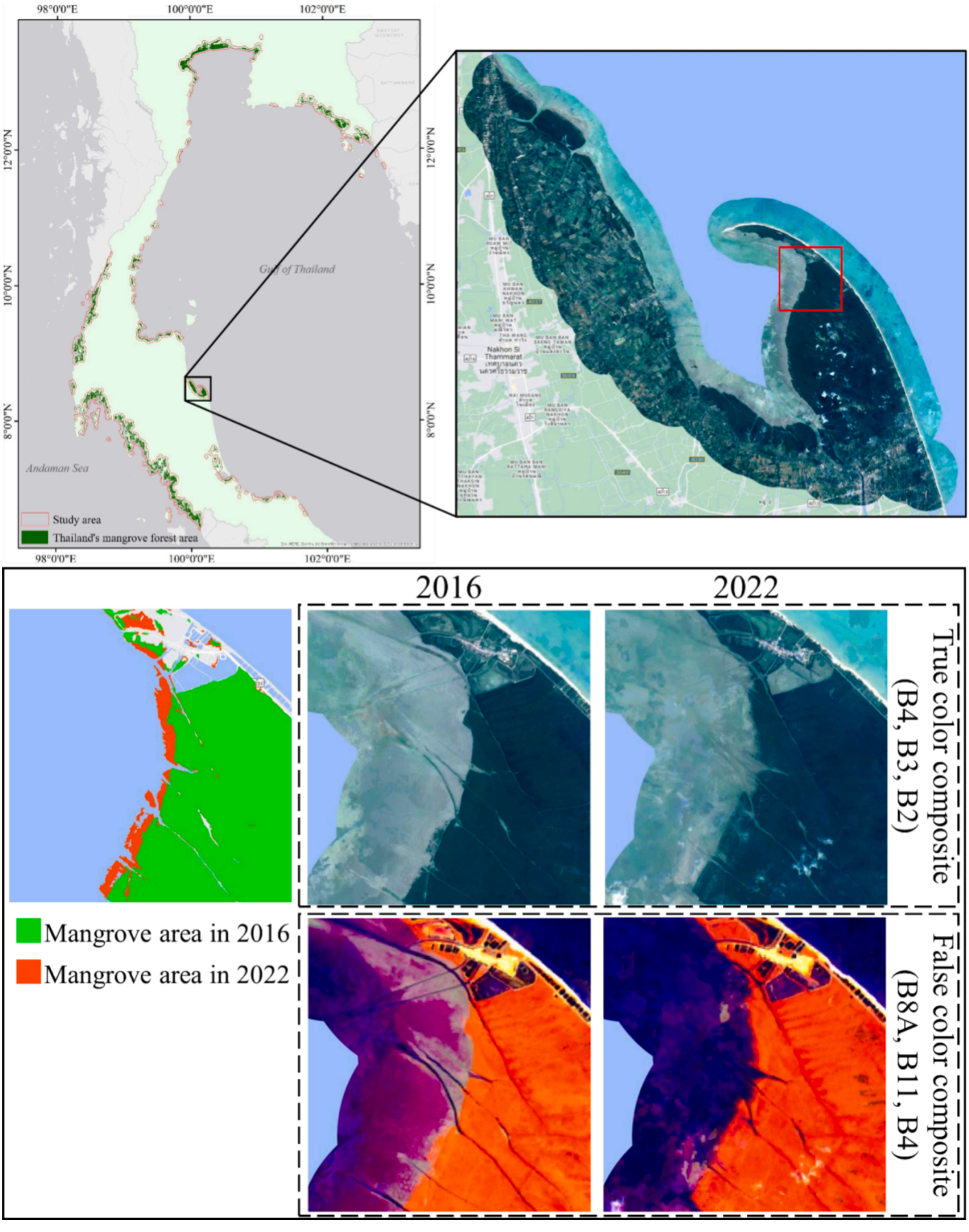


**Fig. 6.** Mangrove coverage around Talumphuk Capein Nakhon Si Thammarat Province. The display illustrates mangroves in 2016 (in green) and their growth by 2022 (in red), complemented by true and false colour composite Sentinel-2 satellite images to corroborate the classification data. (For interpretation of the references to color in this figure legend, the reader is referred to the web version of this article.)

differences in parameters may affect the differences in the results.

## 4. Conclusion

This study resulted in a semi-automated map of Thailand's mangrove areas on a national scale with a spatial resolution of 10 m. The GEE platform enabled the creation of Thailand's mangrove map, integrating remote sensing data from three satellites. Sentinel-1 and Sentinel-2 collectively provide images across complementary spectral bands, offering a comprehensive range of 17 bands. Additionally, SRTM contributes crucial elevation data valuable in analysing mangrove ecosystems where elevation is typically significant. The CART, SVM, RF, and GTB machine learning models were applied to the satellite data to classify the mangrove area in Thailand. All performed relatively well, with the accuracy of the acceptable range: OA (95.43–96.75 %) and Kappa coefficient (0.91–0.94).

GTB is the most accurate, with the highest OA and Kappa coefficient of the ranges on an annual average and across the observed period (2016–2022). GTB also has the lowest IQR, indicating the least sparse in the OA values of yearly data. The one-way ANOVA analysis revealed that GTB's OA is significantly greater than the other models. Therefore, GTB has concluded to be the most adequate model to classify mangrove areas in Thailand.

GTB was utilised in the semi-automated mangrove mapping. Thailand has gained mangrove covers of 11 % during 2016–2022. This finding aligns with the conservation and restoration policies implemented since 2012. Our developed methodology can be used as a guideline for detailed mangrove mapping in other areas and periods on a national or local scale.

## CRediT authorship contribution statement

**Surachet Pinkeaw:** Writing – original draft, Visualization, Validation, Software, Resources, Methodology, Investigation, Funding acquisition, Formal analysis, Data curation. **Pawita Boonrat:** Writing – review & editing, Writing – original draft, Supervision, Project administration. **Werapong Koedsin:** Writing – review & editing, Writing – original draft, Supervision, Conceptualization. **Alfredo Huete:** Writing – review & editing, Writing – original draft, Supervision, Conceptualization.

## Declaration of competing interest

The authors declare that they have no known competing financial interests or personal relationships that could have appeared to influence the work reported in this paper.

## Acknowledgments

The authors would like to thank the Faculty of Technology and Environment, Prince of Songkla University, Phuket Campus, Thailand, and the Study and Sustainable Development for Para Bay and Phang Nga Bay Project by the Electricity Generating Authority of Thailand for their financial support.

## Appendix A. Supplementary data

Supplementary data to this article can be found online at https://doi.org/10.1016/j.ejrs.2024.07.001.

## References

Alongi, D.M., Mukhopadhyay, S.K., 2015. Contribution of mangroves to coastal carbon cycling in low latitude seas. Agric. For. Meteorol. 213, 266–272. https://doi.org/10.1016/j.agrformet.2014.10.005.

Baloloy, A.B., Blanco, A.C., Raymund Rhommel, R.R.C., Nadaoka, K., 2020. Development and application of a new mangrove vegetation index (MVI) for rapid and accurate mangrove mapping. ISPRS J. Photogramm. Remote Sens. 166, 95–117. https://doi.org/10.1016/j.isprsjprs.2020.06.001.

Baviskar, P., Dhiman, R., 2022. Advancing the spatiotemporal assessment of mangrove ecosystem using machine learning approaches-case study of a coastal megacity, Mumbai, India. Earth Sp. Sci. Open Arch.

Bindu, G., Rajan, P., Jishnu, E.S., Ajith Joseph, K., 2020. Carbon stock assessment of mangroves using remote sensing and geographic information system. Egypt. J. Remote Sens. Space. Sci. 23, 1–9. https://doi.org/10.1016/j.ejrs.2018.04.006.

Breiman, L., 2001. Random forests. Mach. Learn. 45, 5–32.

Brown, M.B., Forsythe, A.B., 1974. Robust tests for the equality of variances. J. Am. Stat. Assoc. 69, 364–367.

Bunting, P., Rosenqvist, A., Lucas, R.M., Rebelo, L.M., Hilarides, L., Thomas, N., Hardy, A., Itoh, T., Shimada, M., Finlayson, C.M., 2018. The global mangrove watch - A new 2010 global baseline of mangrove extent. Remote Sens. 10 https://doi.org/10.3390/rs10101669.

Cao, J., Leng, W., Liu, K., Liu, L., He, Z., Zhu, Y., 2018. Object-Based mangrove species classification using unmanned aerial vehicle hyperspectral images and digital surface models. Remote Sens. 10 https://doi.org/10.3390/rs10010089.

Chauhan, S., Srivastava, H.S., 2016. Comparative Evaluation of the Sensitivity of Multi-Polarised Sar and Optical Data for Various Land Cover Classes. Int. J. Adv. Remote Sensing, GIS Geogr. 4, 1–14.

Cissell, J.R., Canty, S.W.J., Steinberg, M.K., Simpson, L.T., 2021. Mapping national mangrove cover for belize using google earth engine and sentinel-2 imagery. Appl. Sci. 11 https://doi.org/10.3390/app11094258.

Cohen, J., 1960. A coefficient of agreement for nominal scales. Educ. Psychol. Meas. 20, 37–46.

Cutler, R., Lawler, J., Thomas Edwards, J., Beard, K.H., Cutler, A., Hess, K.T., Gibson, J., 2007. Random forests for classification in ecology. Ecology 88 (11), 2783–2792.

Department of Marine and Coastal Resources of Thailand (DMCR), 2021a. Mangrove Forest Resources Database System by Mangrove Land Use Classification with High-resolution satellite images Project. DMCR, Bangkok.

Department of Marine and Coastal Resources of Thailand (DMCR), 2021b. Guide to knowledge of mangrove forests. DMCR, Bangkok.

Department of Marine and Coastal Resources of Thailand (DMCR), 2023. State of Marine and Coastal Erosion Thailand National Report 2021. DMCR, Bangkok.

Fernández-Manso, A., Fernández-Manso, O., Quintano, C., 2016. SENTINEL-2A red-edge spectral indices suitability for discriminating burn severity. Int. J. Appl. Earth Obs. Geoinf. 50, 170–175. https://doi.org/10.1016/J.JAG.2016.03.005.

Friedman, J.H., 2002. Stochastic gradient boosting. Comput. Stat. Data Anal. 38, 367–378. https://doi.org/10.1016/S0167-9473(01)00065-2.

Ghorbanian, A., Zaghian, S., Asiyabi, R.M., Amani, M., Mohammadzadeh, A., Jamali, S., 2021. Mangrove ecosystem mapping using sentinel-1 and sentinel-2 satellite images and random forest algorithm in google earth engine. Remote Sens. 13, 1–18. https://doi.org/10.3390/rs13132565.

Giri, C., Pengra, B., Zhu, Z., Singh, A., Tieszen, L.L., 2007. Monitoring mangrove forest dynamics of the Sundarbans in Bangladesh and India using multi-temporal satellite data from 1973 to 2000. Estuar. Coast. Shelf Sci. 73, 91–100. https://doi.org/10.1016/j.ecss.2006.12.019.

Giri, C., Ochieng, E., Tieszen, L.L., Zhu, Z., Singh, A., Loveland, T., Masek, J., Duke, N., 2011. Status and distribution of mangrove forests of the world using earth observation satellite data. Glob. Ecol. Biogeogr. 20, 154–159. https://doi.org/10.1111/j.1466-8238.2010.00584.x.

Giri, C., Long, J., Abbas, S., Murali, R.M., Qamer, F.M., Pengra, B., Thau, D., 2014. Distribution and dynamics of mangrove forests of South Asia. J. Environ. Manage. 148, 101–111. https://doi.org/10.1016/j.jenvman.2014.01.020.

Gorelick, N., Hancher, M., Dixon, M., Ilyushchenko, S., Thau, D., Moore, R., 2017. Google Earth Engine: Planetary-scale geospatial analysis for everyone. Remote Sens. Environ. 202, 18–27. https://doi.org/10.1016/j.rse.2017.06.031.

Hamilton, S.E., Casey, D., 2016. Creation of a high spatio-temporal resolution global database of continuous mangrove forest cover for the 21st century (CGMFC-21). Glob. Ecol. Biogeogr. 25, 729–738. https://doi.org/10.1111/geb.12449.

Hu, L., Qi, C., Wang, Q., 2018. Spectral-spatial hyperspectral image classification based on mathematical morphology post-processing. Procedia Comput. Sci. 129, 93–97. https://doi.org/10.1016/j.procs.2018.03.054.

Hu, L., Xu, N., Liang, J., Li, Z., Chen, L., Zhao, F., 2020. Advancing the mapping of mangrove forests at national-scale using Sentinel-1 and Sentinel-2 time-series data with Google Earth Engine: A case study in China. Remote Sens. 12 https://doi.org/10.3390/RS12193120.

Huete, A.R., 2004. Remote sensing for environmental monitoring. Environ. Monit. Charact. 183–206 https://doi.org/10.1016/B978-012064477-3/50013-8.

Huete, A., Didan, K., Miura, T., Rodriguez, E., Gao, X., Ferreira, L., 2002. Overview of the radiometric and biophysical performance of the MODIS vegetation indices. Remote Sens. Environ. 83, 195–213. https://doi.org/10.1016/S0034-4257(02)00096-2.

Immitzer, M., Vuolo, F., Atzberger, C., 2016. First experience with Sentinel-2 data for crop and tree species classifications in central Europe. Remote Sens. 8 https://doi.org/10.3390/rs8030166.

Li, W., El-Askary, H., Qurban, M.A., Li, J., ManiKandan, K.P., Piechota, T., 2019. Using multi-indices approach to quantify mangrove changes over the Western Arabian Gulf along Saudi Arabia coast. Ecol. Ind. 102, 734–745. https://doi.org/10.1016/j.ecolind.2019.03.047.

Linneweber, V., De Lacerda, L.D., 2002. Mangrove Ecosystems: Function and Management. Springer-Verlag, Berlin, Germany.

Liu, X., Fatoyinbo, T.E., Thomas, N.M., Guan, W.W., Zhan, Y., Mondal, P., Lagomasino, D., Simard, M., Trettin, C.C., Deo, R., Barenblitt, A., 2021. Large-scale high-resolution coastal mangrove forests mapping across West Africa with machine

learning ensemble and satellite big data. Front. Earth Sci. 8, 1–15. https://doi.org/10.3389/feart.2020.560933.
Liu, H.Q., Huete, A., 1995. Feedback based modification of the NDVI to minimize canopy background and atmospheric noise. IEEE Trans. Geosci. Remote Sens. 33, 457–465. https://doi.org/10.1109/36.377946.
Macintyre, P., van Niekerk, A., Mucina, L., 2020. Efficacy oSaengerf multi-season Sentinel-2 imagery for compositional vegetation classification. Int. J. Appl. Earth Obs. Geoinf. 85 https://doi.org/10.1016/j.jag.2019.101980.
Mack, B., Leinenkugel, P., Kuenzer, C., Dech, S., 2017. A semi-automated approach for the generation of a new land use and land cover product for Germany based on Landsat time-series and Lucas in-situ data. Remote Sens. Lett. 8, 244–253. https://doi.org/10.1080/2150704X.2016.1249299.
Mandal, M.S.H., Hosaka, T., 2020. Assessing cyclone disturbances (1988–2016) in the Sundarbans mangrove forests using Landsat and Google Earth Engine. Nat. Hazards 102, 133–150. https://doi.org/10.1007/s11069-020-03914-z.
Miao, J., Zhen, J., Wang, J., Zhao, D., Jiang, X., Shen, Z., Gao, C., Wu, G., 2022. Mapping seasonal leaf nutrients of mangrove with Sentinel-2 images and XGBoost method. Remote Sens. 14 https://doi.org/10.3390/rs14153679.
Mondal, P., Liu, X., Fatoyinbo, T.E., Lagomasino, D., 2019. Evaluating combinations of sentinel-2 data and machine-learning algorithms for mangrove mapping in West Africa. Remote Sens. 11 https://doi.org/10.3390/rs11242928.
Neumann, P., 1997. Salinity resistance and plant growth revisited. Plant Cell Environ. 20, 1193–1198. https://doi.org/10.1046/j.1365-3040.1997.d01-139.x.
Ouma, Y., Nkwae, B., Moalafhi, D., Odirile, P., Parida, B., Anderson, G., Qi, J., 2022. Comparison of machine learning classifiers for multitemporal and multisensor mapping of urban LULC features. Int. Arch. Photogramm. Remote Sens. Spat. Inf. Sci.
Pal, M., Mather, P.M., 2003. An assessment of the effectiveness of decision tree methods for land cover classification. Remote Sens. Environ. 86, 554–565. https://doi.org/10.1016/S0034-4257(03)00132-9.
Persson, M., Lindberg, E., Reese, H., 2018. Tree species classification with multi-temporal Sentinel-2 data. Remote Sens. 10, 1–17. https://doi.org/10.3390/rs10111794.
Pham, T.D., Le, N.N., Ha, N.T., Nguyen, L.V., Xia, J., Yokoya, N., To, T.T., Trinh, H.X., Kieu, L.Q., Takeuchi, W., 2020. Estimating mangrove above-ground biomass using extreme gradient boosting decision trees algorithm with fused sentinel-2 and ALOS-2 PALSAR-2 data in can Gio biosphere reserve, Vietnam. Remote Sens. 12 https://doi.org/10.3390/rs12050777.
Ramoelo, A., Cho, M., Mathieu, R., Skidmore, A.K., 2015. Potential of Sentinel-2 spectral configuration to assess rangeland quality. J. Appl. Remote Sens. 9, 094096 https://doi.org/10.1117/1.jrs.9.094096.
Richards, D.R., Friess, D.A., 2016. Rates and drivers of mangrove deforestation in Southeast Asia, 2000–2012. Proc. Natl. Acad. Sci. 113, 344–349. https://doi.org/10.1073/pnas.1510272113.
Sarzynski, T., Giam, X., Carrasco, L., 2020. Combining Radar and Optical Imagery to Map Oil Palm Plantations in Sumatra , Indonesia , Using the Google Earth Engine.
Sharma, S., Paul, A., Mitra, D., Chauhan, P., 2021. Semi-automated workflow for mapping the extent and elevation profile of intertidal zone of parts of Gulf of Kutch, India, using Landsat Time Series Data. J. Indian Soc. Remote Sens. 49, 1343–1363. https://doi.org/10.1007/s12524-020-01291-5.
Shelestov, A., Lavreniuk, M., Kussul, N., Novikov, A., Skakun, S., 2017. Exploring Google Earth Engine platform for big data processing: Classification of multi-temporal satellite imagery for crop mapping. Front. Earth Sci. 17.
Shiau, Y.J., Lee, S.C., Chen, T.H., Tian, G., Chiu, C.Y., 2017. Water salinity effects on growth and nitrogen assimilation rate of mangrove (Kandelia candel) seedlings. Aquat. Bot. 137, 50–55. https://doi.org/10.1016/j.aquabot.2016.11.008.
Singh, A., Mahajan, S., 2023. Classification and above ground biomass mapping of Indian landlocked mangrove forest through Sar data. Ann. For. Res. 66, 3114–3142.
Sun, L., Chen, J., Guo, S., Deng, X., Han, Y., 2020. Integration of time series sentinel-1 and sentinel-2 imagery for crop type mapping over oasis agricultural areas. Remote Sens. 12 https://doi.org/10.3390/RS12010158.
Tamiminia, H., Salehi, B., Mahdianpari, M., Quackenbush, L., Adeli, S., Brisco, B., 2020. Google Earth Engine for geo-big data applications: A meta-analysis and systematic review. ISPRS J. Photogramm. Remote Sens. 164, 152–170. https://doi.org/10.1016/j.isprsjprs.2020.04.001.
The Ministry of Natural Resources and Environment, 2021. 20-year Master Plan of the Ministry of Natural Resources and Environment (2018-2037). The Ministry of Natural Resources and Environment, Bangkok.
The National Economic and Society Development Board, 2011. 11th National Economic and Social Development Plan (2012-2016). The National Economic and Society Development Board, Bangkok.
The National Economic and Society Development Board, 2016. 12th National Economic and Social Development Plan (2017-2021). The National Economic and Society Development Board, Bangkok.
Thomas, N., Lucas, R., Bunting, P., Hardy, A., Rosenqvist, A., Simard, M., 2017. Distribution and drivers of global mangrove forest change, 1996–2010. PLoS One 12, 1–14. https://doi.org/10.1371/journal.pone.0179302.
Tian, Y.-C., Jia, K., Wu, B.-F., Li, Q.-Z., 2010. Study on spectral reflectance characteristics of hemp canopies. Spectrosc. Spectr. Anal. 30, 3334–3337.
Toosi, N.B., Soffianian, A.R., Fakheran, S., Pourmanafi, S., Ginzler, C., Waser, L.T., 2019. Comparing different classification algorithms for monitoring mangrove cover changes in southern Iran. Glob. Ecol. Conserv. 19 https://doi.org/10.1016/j.gecco.2019.e00662.
Wu, Z., Snyder, G., Vadnais, C., Arora, R., Babcock, M., Stensaas, G., Doucette, P., Newman, T., 2019. User needs for future Landsat missions. Remote Sens. Environ. 231, 111214 https://doi.org/10.1016/j.rse.2019.111214.
Xia, Q., Qin, C.Z., Li, H., Huang, C., Su, F.Z., 2018. Mapping mangrove forests based on multi-tidal high-resolution satellite imagery. Remote Sens. 10 https://doi.org/10.3390/rs10091343.
Yang, G., Huang, K., Sun, W., Meng, X., Mao, D., Ge, Y., 2022. Enhanced mangrove vegetation index based on hyperspectral images for mapping mangrove. ISPRS J. Photogramm. Remote Sens. 189, 236–254. https://doi.org/10.1016/j.isprsjprs.2022.05.003.
Zhang, C., Kovacs, J.M., Liu, Y., Flores-Verdugo, F., Flores-de-Santiago, F., 2014. Separating mangrove species and conditions using laboratory hyperspectral data: A case study of a degraded mangrove forest of the Mexican Pacific. Remote Sens. 6, 11673–11688. https://doi.org/10.3390/rs61211673.
Zhao, C., Qin, C.Z., 2020. 10-m-resolution mangrove maps of China derived from multi-source and multi-temporal satellite observations. ISPRS J. Photogramm. Remote Sens. 169, 389–405. https://doi.org/10.1016/j.isprsjprs.2020.10.001.
Zhu, B., Liao, J., Shen, G., 2021. Combining time series and land cover data for analyzing spatio-temporal changes in mangrove forests: A case study of Qinglangang Nature Reserve, Hainan, China. Ecol. Indic. 131, 108135 https://doi.org/10.1016/j.ecolind.2021.108135.